

# Design and Tuning of PID Override Control System Based on Signal Filtering

Aleksandar I. Ribić

Institute Mihajlo Pupin,  
Belgrade, Serbia  
e-mail: aleksandar.ribic@pupin.rs

Miroslav R. Mataušek

Faculty of Electrical Engineering,  
University of Belgrade  
Belgrade, Serbia  
e-mail: matausek@etf.rs

**Abstract**— The proposed override control system consists of two anti-reset windup controllers, common actuator and a limiter, surrounded by pre and post biproper filters. Pre-filter is inverse of the post-filter. The desired limit on the override variable and its set-point are defined by output of the limiter. Signal selector is not applied in the proposed structure. Other characteristic feature of the proposed solution, compared to standard one, is that the override variable response is obtained practically without overshoot. Procedure for adjusting parameters of the post-filter are defined and illustrated in detail. Simulation results are used to demonstrate the basic ideas. Experiment on a laboratory thermal plant with noisy measurements is used to confirm validity of the proposed solution.

**Keywords**—PID control; Override control; Constraints; Dead-time compensation; Tuning

## I. INTRODUCTION

In many cases the number of variables to be controlled is higher than the number of manipulated variables. Override and cascade control are commonly applied to solve this control problem at the regulatory control level. In the present paper a new, effective solution for override control system design and tuning is proposed and experimentally verified.

In override control, one variable is a primary controlled variable  $y_p$  and have to be maintained at a given reference value  $r_p$  (or close as much as possible), but in such way that the override variable  $y_o$  had to be limited to a value  $r_o$ , defined in [1] as the soft constraint.

Block diagram of a standard override controller is presented in Fig. 1. Actuator output  $w$  is used as external reset feedback, common to both anti-reset windup controllers  $C_p$  and  $C_o$ . Two controller outputs are connected to a signal selector (min or max). The controller demanding higher or lower actuator output  $w$  will override the other. In the normal operating regime, this controller is the primary one,  $C_p$ . Stability of this standard override control system is considered in [2].

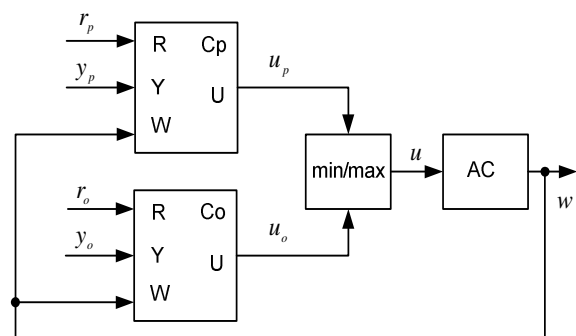


Figure 1. Block diagram of a standard override control system: primary controller  $C_p$  and override controller  $C_o$  connected to the common actuator AC through the min/max selector.

Suppose that primary  $y_p$  and override  $y_o$  variables are defined by  $y_p = G_p w$  and  $y_o = G_o w$ , where  $G_p$  and  $G_o$  are some process transfer functions. It is adopted that the selector in Fig. 1 is of a min type. In this case, when override variable  $y_o$  approaches closely to its limit  $r_o$ , then output signal  $u_o$  decreases. When it drops below the primary controller's output  $u_p$ , it is selected as actuator input  $u$ . This means that the controller  $C_o$  overrides the primary controller  $C_p$ , as demonstrated in Fig. 2 for the example with process transfer functions  $G_p$  and  $G_o$  defined by:

$$G_p(s) = \frac{e^{-0.2s}}{s}, G_o(s) = \frac{10e^{-s}}{10s+1}, \quad (1)$$

and anti-reset windup PI controller used for the primary controller  $C_p$  and override controller  $C_o$ , defined in Section 2.

The basic problem with the override control in Fig. 1 is the overshoot in  $y_o$  response following the set-point  $r_p$  change. This is demonstrated in Fig. 3, for the above example defined by (1) and Fig. 1.

Appearance of overshoot in Fig. 3 reduces performance of override control. This conclusion follows from the fact that the override set-point  $r_o$  (soft constraint) has to be set sufficiently far from the interlock trip point, denoted in [1] as the hard constraint.

In the present paper a new structure of the override control system is proposed in Section II. It enables to solve efficiently the above overshoot problem in the case of set-point  $r_p$  change as well as in the presence of disturbances.

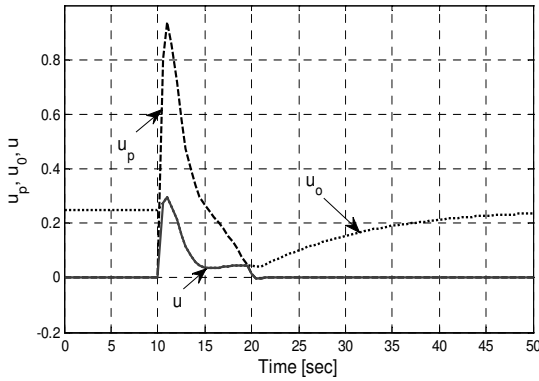


Figure 2. Control signals  $u_p$  (dashed),  $u_o$  (dotted) and resulting  $u$  (solid) of override control system in Fig. 1, with selector of a min type.

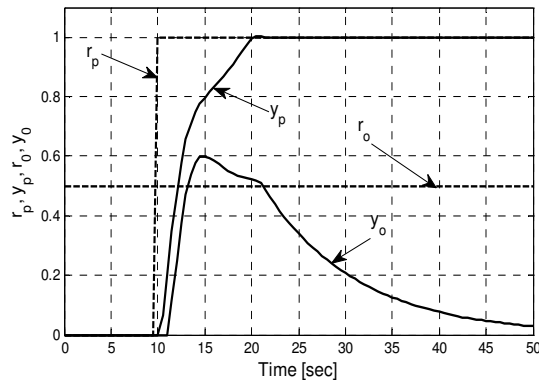


Figure 3. Set-point (dashed) and process output (solid) responses of override control system in Fig. 1. Standard override controller  $C_o$  can not prevent appearance of overshoot in the override variable  $y_o$ .

Design and tuning of the proposed override control system is presented in Section III. Then, for a laboratory thermal plant with noisy measurements, in Section IV the basic ideas are illustrated by simulation, and experimental results are used for final verification.

## II. PROPOSED STRUCTURE

The proposed override control system is presented in Fig. 4. The characteristic feature of the proposed structure is the limiter surrounded with a biproper post-filter and its inverse, a pre-filter. Polynomial  $A_2(s)$  is given by  $A_2(s)=a_2s^2+a_1s+a_0$ ,  $F_n(s)=1/(T_n s+1)^n$  is an  $n^{\text{th}}$  order low-pass filter,  $n \geq 1$ , and  $L$  is a design parameter [3,4]. The same structure is used for the primary controller, with  $F_r(s) \equiv F_n(s)$ . Obviously, first-order filter  $F_n(s)$  can be applied for  $a_2=0$ , as in Table I.

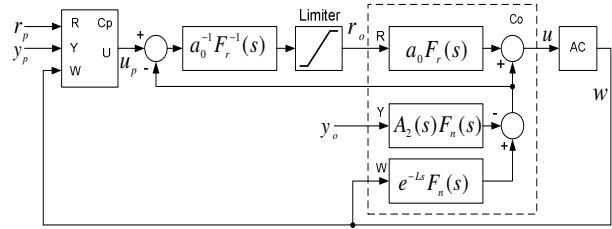


Figure 4. Proposed override control system: primary controller  $C_p$  and override controller  $C_o$  connected to the common actuator AC. Inside limits  $u(t) \equiv u_p(t)$  and override controller  $C_o$  is inactive.  $F_r(s)$  is a biproper post-filter with  $F_r(0)=1$ .

The proposed mechanism is simple and obvious. As the pre-filter is used to be inverse of biproper post-filter, inside limits one obtains  $u(t) \equiv u_p(t)$  since the action of the override controller  $C_o$  in Fig. 4 is cancelled. When the set-point  $r_o(t)$  reaches the limit, the connection relating primary controller to actuator is broken and override controller  $C_o$  is active with set-point defined by a desired limit.

The proposed structure is applied to the above example (1). To demonstrate advantages of the proposed override control system, the same PI controllers ( $a_2=0, L=0, n=1$ ) are used in the standard override control system, with results presented in Figs. 2-3, and in the proposed structure, used to obtain results in Fig. 5. Parameters of PI controllers are given in Table I.

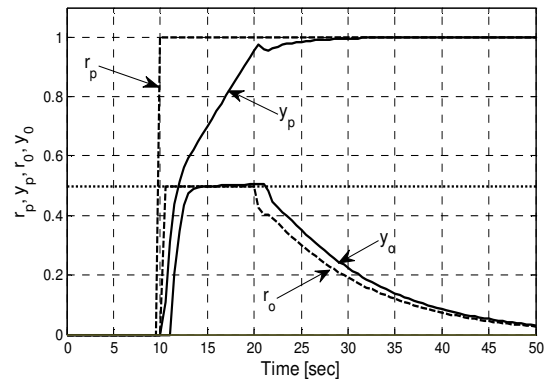


Figure 5. Set-point (dashed) and process output (solid) responses of the proposed override control system in Fig. 4. Dot line presents the desired limit for  $y_o$ .

TABLE I. PARAMETERS OF APPLIED PI CONTROLLERS

Controller	$a_0$	$a_1$	$T_i$
Override	0.5	2.5	5
Primary	1.25	1.25	0.5

Results presented in Fig. 5 confirm that the desired limit is almost strictly satisfied, by using the proposed override control system and the post-filter tuning derived in the next section.

### III. DESIGN OF THE POST-FILTER

Assume that both controllers in Fig. 4 are tuned to satisfy some desired performance/robustness trade-off, for a given dynamic process characterization  $y_p=G_p w$  and  $y_o=G_o w$  defined by transfer functions  $G_p$  and  $G_o$ . This means that the post-filter  $F_r(s)$  in Fig. 4 is designed assuming that  $G_o$  and controllers  $C_p$  and  $C_o$  are known.

Set-point response of  $y_o$  is defined by transfer function

$$G_{ro}(s) = \frac{Y_o(s)}{R_o(s)} = \frac{a_0 G_o(s)}{1 + F_n(s)(A_2(s)G_o(s) - e^{-Ls})}, \quad (2)$$

for  $F_r(s) \equiv 1$ . To obtain fast set-point response of  $y_o$  without the overshoot, the ideal form of the post-filter is obtained as the inverse of  $G_{ro}(s)$ . However, this implementation is not always possible, and it is proposed to use a rational function approximation of  $G_{ro}(s)$ . Since  $G_{ro}(0)=1$ , this approximation is given by

$$G_{ro}(s) \approx \frac{1+C(s)}{1+D(s)}, C(s) = \sum_{i=1}^n c_i s^i, D(s) = \sum_{i=1}^q d_i s^i, p \leq q. \quad (3)$$

Coefficients of polynomials  $C(s)$  and  $D(s)$  are determined by minimizing the following criteria

$$\min_{c_m, d_m} \sum_{k=1}^K \left| \frac{1+D_m(i\omega_k)}{1+D_{m-1}(i\omega_k)} G_{ro}(i\omega_k) - \frac{1+C_m(i\omega_k)}{1+D_{m-1}(i\omega_k)} \right|^2, m = 1, 2, \dots, N, \quad (4)$$

performed through iterations, for  $D_0(i\omega_k) \equiv 0$  and  $\omega_k \in \Omega$ ,  $\Omega = \{\omega_1, \omega_2, \dots, \omega_K\}$ , where  $\Omega$  is a set of frequencies in the desired range. It should be observed that from (4) one obtains  $G_{ro}(i\omega_k) \approx (1+C_N(i\omega_k))/(1+D_N(i\omega_k))$  for  $\omega_k \in \Omega$ , as required by (3), since for  $m=N$  it follows  $D_{m-1}(i\omega_k) \approx D_m(i\omega_k)$ .

Poles and zeros of  $(1+C_N(s))/(1+D_N(s))$  in the left half  $s$ -plane, close to the imaginary axes, are used to approximate dominant dynamics of  $G_{ro}(s)$ . Right Half  $s$ -Plane (RHP) zeros are excluded. Then, the biproper post-filter  $F_r(s)$  is designed as the inverse of dominant dynamics of  $G_{ro}(s)$ . To obtain the biproper post-filter  $F_r(s)$  in the form

$$F_r(s) = \frac{1+B_r(s)}{1+A_r(s)}, B_r(s) = \sum_{i=1}^m b_i s^i, A_r(s) = \sum_{i=1}^m a_i s^i, \quad (5)$$

some additional zeros  $(T_z s + 1)^g$ , defined by time constant  $T_z$  and order  $g$ , have to be included in polynomial  $1+B_r(s)$ , to obtain the same order  $m$  of  $B_r(s)$  and  $A_r(s)$  in (5). Further details will be demonstrated here and in the next section.

For the example (1), the following approximation of  $G_{ro}(s)$  is obtained from (4):

$$\frac{1+C(s)}{1+D(s)} = \frac{(1-1.0977s)(4.1271s+1)}{(2.7988s+1)(1.2291s^2+1.7552s+1) \cdot \frac{(0.0395s^2-0.1692s+1)}{(0.0308s^2+0.1725s+1)}}.$$

The biproper post-filter  $F_r(s)$ , with time constant  $T_z=0.5$  s, adopted as a trade-off between the performance and the high-frequency gain  $F_r(\infty)$ , is given by

$$F_r(s) = \frac{(2.7988s+1)(1.2291s^2+1.7552s+1)}{(4.1271s+1)(0.5s+1)^2}.$$

### IV. SIMULATION AND EXPERIMENTAL RESULTS

A laboratory thermal plant, with noisy measurements, is used to demonstrate in detail the basic ideas and properties of the proposed solution and to verify experimentally the validity of the override control system in Fig. 4. In this section, DTC-PID controllers [3,4] are used as primary and override controller in the proposed override control system.

The plant is presented in Fig. 6. The temperature  $T(x,t)$  of aluminum plate, long  $l=0.1$  m and wide  $h=0.03$  m, is measured by precision sensors LM35 (TO92) at positions  $x=0$  and  $x=l$ . The plate is heated by terminal adjustable regulator LM317 (TO 220) at  $x=0$ . The input to the heater is the manipulated variable  $w(t)$ , obtained from the saturation element with limits  $l_{low}=0\%$  and  $l_{high}=100\%$  [4]:

$$w(t) = \begin{cases} u(t), & l_{low} < u(t) < l_{high} \\ l_{low}, & u(t) \leq l_{low} \\ l_{high}, & u(t) \geq l_{high} \end{cases}. \quad (6)$$

The primary controlled variable is  $y_p(t)=T(l,t)$  [ $^{\circ}\text{C}$ ], while measurement at the position  $x=0$  of the heater is used as the override variable  $y_o(t)=T(0,t)$ , to keep the temperature  $T(0,t)$  below  $59^{\circ}\text{C}$ .

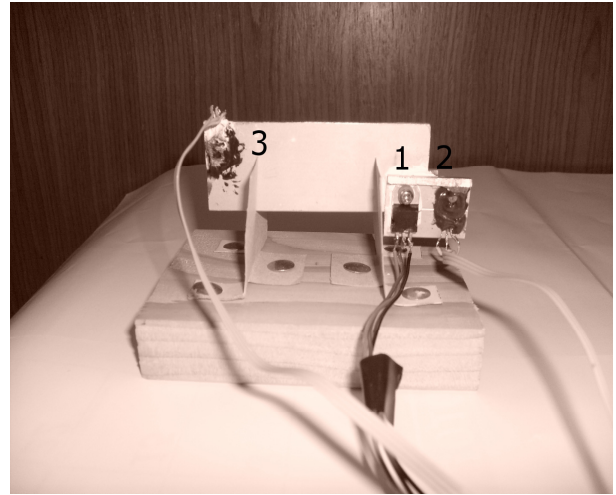


Figure 6. Laboratory thermal plant: 1- heater, 2- sensor at  $x=0$ , 3- sensor at  $x=l$ .

For the nominal regime, defined by the  $T(l,t) \approx 50^{\circ}\text{C}$ , the open-loop system responses of both outputs  $y_p(t)$  and  $y_o(t)$ , obtained by applying a PRBS signal  $w(t)$ , are used to determine 100<sup>th</sup>-order ARX models, approximated then with the following models  $y_p=G_p w$  and  $y_o=G_o w$ :

$$G_p(s) = \frac{1.375(3.627s+1)(1-1.295s)}{(580.05s+1)(4.85s+1)(3.24s+1)(201.13s^2+25.52s+1)},$$

$$G_o(s) = \frac{1.609(53.079s+1)(2.064s+1)}{(503s+1)(26.62s+1)(7.21s+1)(1.88s+1)(1.83s+1)}. \quad (7)$$

Both DTC-PID controllers are defined by the structure of the override controller in Fig. 4, with  $F_r(s) \equiv F_n(s)$  used in the primary controller, as in [4]. In both controllers fourth-order filter  $F_n(s) = 1/(T_f s + 1)^4$  is used. Parameters of DTC-PID controllers in Table II are obtained by optimization under constraints on the robustness and sensitivity to measurement noise [4].

TABLE II. PARAMETERS OF APPLIED DTC-PID CONTROLLERS

Controller	$a_0$	$a_1$	$a_2$	$T_i$	$L$
Override	14.276	265.983	1649.6	2.2191	0.1493
Primary	10.906	730.446	12785	5.0806	17.569

The following approximation of  $G_{ro}(s)$  is obtained from (4):

$$\frac{1+C(s)}{1+D(s)} = -0.0002295 \frac{(s-4.676)(s+0.01946)}{(s+2.167)(s+0.02023)} \cdot \frac{(s^2+0.4557s+0.06945)(s^2-0.737s+14.15)}{(s^2+0.1209s+0.008719)(s^2+0.2194s+0.0537)}. \quad (8)$$

Frequency responses of  $G_{ro}(s)$  in (2) are used to define the desired range of frequencies  $\omega_k \in \Omega$ . It is proposed to use set of frequencies where amplitude characteristic of  $G_{ro}(s)$  is greater than -60dB. Frequency responses of  $G_{ro}(s)$  in (2), and its approximation (8), are presented in Fig. 7.

Filter  $F_r(s)$  is obtained by applying design procedure (4)-(5) and taking into account only dominant poles and zeros of approximation (8). RHP zero  $s=4.576$  and non-dominated pole  $s=-2.167$  are neglected. Then, RHP zeros defined by  $(s^2-0.737s+14.15)=0$  are neglected, and this term is replaced with  $(7s+1)^2$  to obtain biproper  $F_r(s)$  defined by:

$$F_r(s) = \frac{1+B(s)}{1+A(s)} = \frac{(49.4315s+1)}{(51.3875s+1)} \cdot \frac{(114.6921s^2+13.8663s+1)(18.622s^2+4.0857s+1)}{(14.398s^2+6.5616s+1)(7s+1)^2}. \quad (9)$$

Time constant  $T_z=7$  s is adopted as a trade-off between the performance and high-frequency gain, to obtain  $F_r(\infty) \approx 3$  as in the previous example with responses presented in Fig. 5.

Simulation of the laboratory thermal plant is performed first, by applying models  $G_p(s)$  and  $G_o(s)$  in (7) in the loop with the proposed override control system defined by Fig. 4, Table II and post-filter (9).

Results of this simulation, presented in Fig. 8, are obtained as follows. Limit for  $y_o(t)$  is set to  $r_{\text{omax}}=6.5$  °C. A band-limited white noise is added to both variables,  $y_p(t)$  and  $y_o(t)$ . It is obtained from a band-limited white noise generator, with power PSD=0.0015 and cut-off frequency  $\omega_c=\pi/0.5$  rad/s.

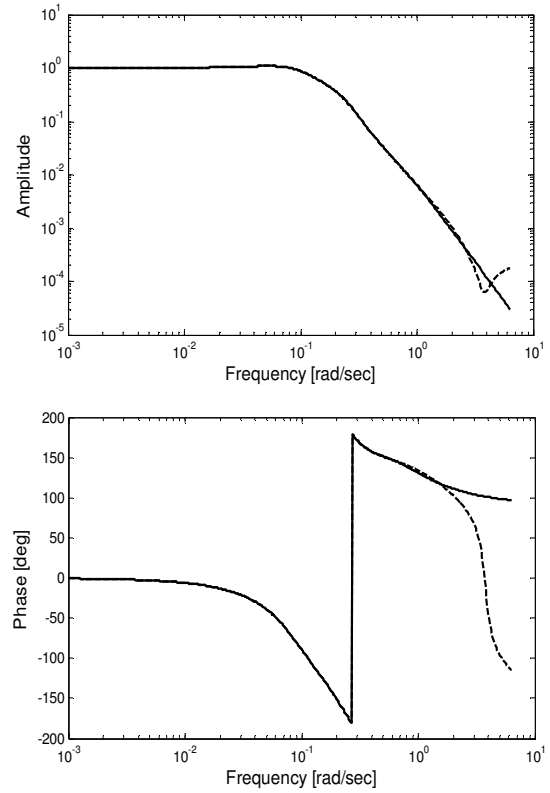


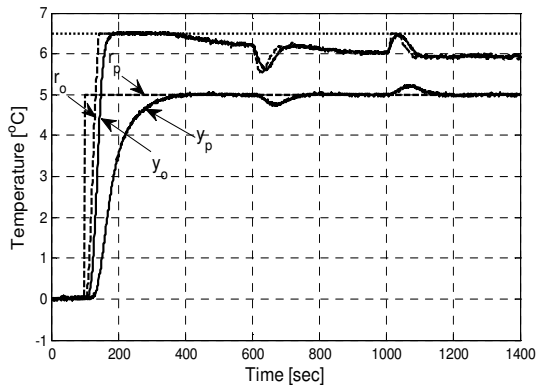
Figure 7. Frequency responses of  $G_{ro}(s)$  (solid) and its approximation  $(1+C(s))/(1+D(s))$  (dashed), obtained for  $p=q=6$  in (3).

A step set-point  $r_p(t)$  of amplitude 5 °C is activated at  $t=100$  s. The set-point  $r_o(t)$  is generated, followed by the override variable  $y_o(t)$ , regardless the fact that the override controller is inactive until  $r_o(t)$  becomes equal to the desired limit. When  $r_o(t)$  becomes equal to the desired limit, action of the override controller provides that the desired limit on override variable is strictly satisfied, as demonstrated in Fig. 8a.

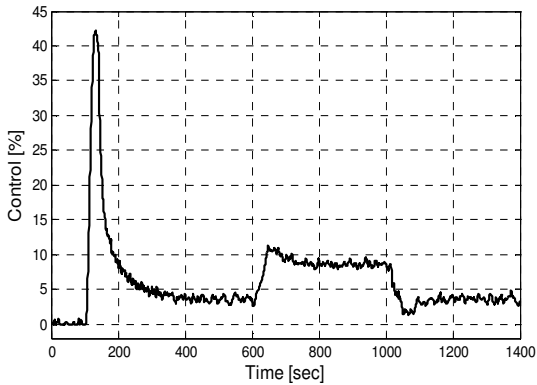
To illustrate performance of the proposed override control system in the presence of an unmeasurable load disturbance, a -5% step change of the control variable is inserted at time  $t=600$  s and deactivated at  $t=1000$  s.

Results of experimental verification of the proposed override control system in the loop with the real laboratory thermal plant are presented in Fig. 9. As in the simulation, set-point change of the primary variable equals 5 °C, from the nominal value of 45 °C.

In this case, limit on  $y_o(t)$ , given by  $r_{\text{omax}}=59$  °C, and the new operating point are adjusted to demonstrate performance of the proposed override control in the vicinity of the desired limit. In the presence of unmeasurable disturbances, the desired override limit is not exceeded due to fast reaction of the override controller, as demonstrated in Fig. 9a.



a)



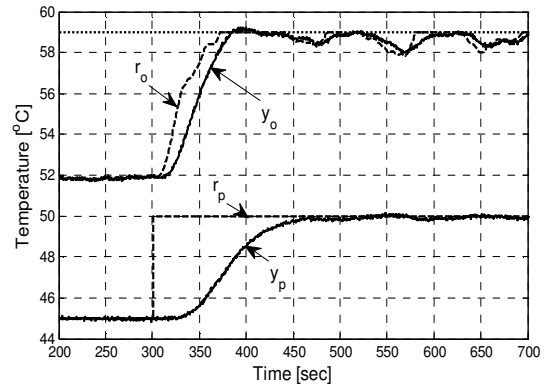
b)

Figure 8. Closed-loop simulation of the laboratory thermal plant, models  $G_p(s)$  and  $G_o(s)$  in (7) in the loop with the proposed override control system in Fig. 4: a) Set-points  $r_o(t)$  and  $r_p(t)$  (dashed),  $y_o(t)$  and  $y_p(t)$  (solid), and desired limit for  $y_o(t)$  (dotted); b) control  $w(t)$ . A step change of control is activated at  $t=600$  s and deactivated at  $t=1000$  s.

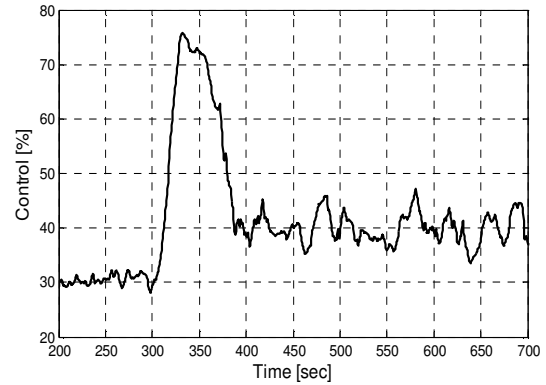
## V. CONCLUSIONS

Advances in PID like control algorithms are still of great importance, since, as demonstrated in [5] and confirmed recently in [6], PID controller still predominates on the regulatory control level. The proposed override controller offers an effective mechanism to deal with constraints in actuator and constraints on the process outputs at the regulatory control level. Tuning of this override controller is defined by the proposed tuning of the filter  $F_r(s)$ , taking into account that tuning procedures for PID and DTC-PID controllers are defined in the available literature.

Set-point filters are mostly applied to avoid abrupt changes of controlled and control variables. However, there are examples when a fast reaction on the set-point obtained from higher control levels is required and constraints on controlled and control variables allow such implementation. In these cases, a desired set-point following performance can be obtained if the procedure proposed to design and tune filter  $F_r(s)$  is applied to define set-point filters for controllers on the regulatory control level.



a)



b)

Figure 9. Responses of the laboratory thermal plant in the loop with the proposed override controller. At  $t=300$  s the set-point  $r_p(t)$  is changed from 45 °C to 50 °C: a) Set-points  $r_o(t)$  and  $r_p(t)$  (dashed),  $y_o(t)$  and  $y_p(t)$  (solid), and desired limit for  $y_o(t)$  (dotted); b) control  $w(t)$ . The desired override limit is not exceeded in the presence of unmeasurable disturbances.

Finally, in cascade control systems, a limiter is frequently applied on the inner loop set-point to keep the secondary output below the safety limit. In this case, the procedure proposed to design and tune filter  $F_r(s)$  can be directly applied to avoid the overshoot. This is important to avoid action of safety devices, very costly to plant operation.

## ACKNOWLEDGMENT

A.I. Ribić gratefully acknowledges the financial support from Serbian Ministry of Science and Technology (Project TR33022 and TR35003).

## REFERENCES

- [1] F.G. Shinskey, J.P. Shunta, J.E. Jamison, and A. Rohr, "Selective, Override, and Limit Controls", in *Process Control and Optimization*, 4th ed., vol. II, Béla Lipták Ed, CRC Press, Boca Raton, 2006, pp.336-344.
- [2] A.H. Glatfelter, W. Schaufelberger, "Stability of discrete override and cascade-limiter single-loop control systems", *IEEE Trans. on Automatic Control*, pp. 532-540, 1998.
- [3] A.I. Ribić, "Development of a new industrial controller: structure, models, tuning and implementation on thermal power plants", Ph.D.Thesis (in Serbian), University of Belgrade, Faculty of Electrical Engineering, Serbia, 2010.

- [4] A.I. Ribić, M.R. Mataušek, "A dead-time compensating PID controller structure and robust tuning", *Journal of Process Control* pp.1340-1349, 2012.
- [5] L. Desborough, R. Miller, "Increasing customer value of industrial control performance monitoring-Honeywell's experience", 6th. Int. Conf. on Chemical Process Control, 2002, AIChE Symp. Series Number 326, vol. 98.
- [6] M. Kano, M. Ogawa, 2010. "The state of the art in chemical process control in Japan: Good practice and questionnaire survey", *Journal of Process Control* pp 969-982, 2010.